The Dynamic Correlation Model and Its Application to the Heston Model

L. Teng, M. Ehrhardt and M. Günther

Abstract Correlation plays an essential role in many problems of finance and economics, such as pricing financial products and hedging strategies, since it models the degree of relationship between, e.g., financial products and financial institutions. However, usually for simplicity the correlation coefficient is assumed to be a constant in many models, although financial quantities are correlated in a strongly nonlinear way in the real market. This work provides a new time-dependent correlation function, which can be easily used to construct dynamically (time-dependent) correlated Brownian motions and flexibly incorporated in many financial models. The aim of using our time-dependent correlation function is to reasonably choose additional parameters to increase the fitting quality on the one hand, but also add an economic concept on the other hand. As examples, we illustrate the applications of dynamic correlation in the Heston model. From our numerical results we conclude that the Heston model extended by incorporating time-dependent correlations can provide a better volatility smile than the pure Heston model.

Keywords Time-dependent correlations · Heston model · Implied volatility · Nonlinear dependence

1   Introduction

Correlation is a well-established concept for quantifying interdependence. It plays an essential role in several problems of finance and economics, such as pricing financial

L. Teng (✉) · M. Ehrhardt · M. Günther
Lehrstuhl für Angewandte Mathematik und Numerische Analysis,
Fakultät Mathematik und Naturwissenschaften, Bergische Universität
Wuppertal, Gaußstr. 20, 42119 Wuppertal, Germany
e-mail: teng@math.uni-wuppertal.de

M. Ehrhardt
e-mail: ehrhardt@math.uni-wuppertal.de

M. Günther
e-mail: guenther@math.uni-wuppertal.de

products and hedging strategies. For example, in [3] the arbitrage pricing model is based on that correlation as a measure for the dependence among the assets, and in portfolio credit models the default correlation is one fundamental factor of risk evaluation, see [1, 2, 12].

In most of the financial models, the correlation has been considered as a constant. However, this is not a realistic assumption due to the well-known fact that the correlation is hardly a fixed constant, see e.g. [7, 13]. For example, in many situations the pure Heston model [9] cannot provide enough skews or smiles in the implied volatility surface as market requires, especially for a short maturity. A reason for this might be that deterministically correlated Brownian motions (BMs) of the price process and the variance process are used, as the correlation mainly affects the slope of implied volatility smile. If the correlation is modeled as a time-dependent dynamic function, better skews or smiles will be provided in the implied volatility surface by reasonably choosing additional parameters. Furthermore, compared with the way to extend a model by using time-dependent parameter, e.g., [6, 10] for the Heston model, a time-dependent correlation function adds an economic concept (nonlinear relationship) and its application will be considerably simpler.

The key of modeling correlation as a time-dependent function is being able to ensure that the boundaries -1 and 1 of the correlation function are not attractive and unattainable for any time. In this work, we build up a appropriate time-dependent correlation function, so that one can reasonably choose additional parameters to increase the fitting quality on the one hand but also add an economic concept on the other hand.

The outline of the remaining part is as follows. Section 2 is devoted to a specific dynamic correlation function and its (analytical) computation. In Sect. 3, we present the concept of dynamically (time-dependent) correlated Brownian motions and the corresponding construction. The incorporation of our new dynamic correlation model in the Heston model is illustrated in Sect. 4. Finally, in Sect. 5 we conclude.

2   The Dynamic Correlation Function

In this section we introduce a dynamic correlation function. Actually, it is in high demand to find such a correlation function which must satisfy the correlation properties: it provides only the values in the interval $(-1, 1)$ for any time; it converges for increasing time. We find the following simple idea: we denote the dynamic correlation by $\bar{\rho}$ and propose simply using

$$\bar{\rho}_t := E\left[\tanh(X_t)\right], \quad t > 0 \tag{1}$$

for the *dynamic correlation function,* where X_t is any mean-reverting process with positive and negative values. For the known parameters of X_t, the correlation function $\bar{\rho}_t : [0, t] \to (-1, 1)$ depends only on t. We observe that the dynamic correlation model (1) satisfies the desired properties: first, it is obvious that $\bar{\rho}_t$ takes values only

in $(-1, 1)$ for all t. Besides, it converges for increasing time due to the mean reversion of the used process X_t.

Although we could intuitively observe that the function tanh is eminently suitable for transforming value to the interval $(-1, 1)$, one might still ask whether other functions can also be applied for this purpose, like trigonometric functions or $\frac{2}{\pi} \arctan(\frac{\pi}{2}x)$. In theory, such functions could be used for this purpose. However, the problem is whether one can obtain the expectation of the transformed mean-reverting process by such functions in a closed-form expression. Furthermore, our experiments show that the tendency of the function tanh is more suitable for modeling correlations, see [13].

X_t in (1) could be any mean-reverting process which allows positive and negative outcomes. As an example, let X_t be the *Ornstein–Uhlenbeck process* [14]

$$dX_t = \kappa(\mu - X_t)dt + \sigma dW_t, \quad t \geq 0. \tag{2}$$

We are interested in computing $E[\bar{\rho}_t]$ as a function of the given parameters in (2). We compute $\bar{\rho}_t = E[\tanh(X_t)]$ as

$$\bar{\rho}_t = E[\tanh(X_t)] = E\left[1 - e^{-X_t} \cdot \frac{2}{e^{-X_t} + e^{X_t}}\right] = 1 - E\left[e^{-X_t} \cdot \frac{1}{\cosh(X_t)}\right]. \tag{3}$$

We set $g(X_t) = 1/\cosh(X_t)$. Applying the results by Chen and Joslin [4], the expectation in (3) can be found in closed-form expression (up to an integral) as

$$\frac{1}{2\pi} \int_{-\infty}^{\infty} \hat{g}(u) \cdot E[e^{-X_t} e^{iuX_t}] \, du, \tag{4}$$

where $i = \sqrt{-1}$ denotes the imaginary unit and $\hat{g}$ is the Fourier transform of g, in this case is known analytically by $\hat{g}(u) = \pi/\cosh(\frac{\pi u}{2})$. Denoting $CF(t, u|X_0, \kappa, \mu, \sigma)$ as the characteristic function of X_t, the expectation in (4) can be presented by $CF(t, i + u|X_0, \kappa, \mu, \sigma)$. Thus, we obtain the closed-form expression for $\bar{\rho}_t$:

$$\bar{\rho}_t = 1 - \frac{1}{2} \int_{-\infty}^{\infty} \frac{1}{\cosh(\frac{\pi u}{2})} \cdot CF(t, i + u|X_0, \kappa, \mu, \sigma) du. \tag{5}$$

The next step is to calculate $CF(t, i + u|X_0, \kappa, \mu, \sigma)$. The process X_t is an Ornstein–Uhlenbeck process and its characteristic function $CF(t, u|X_0, \kappa, \mu, \sigma)$ can be obtained analytically, e.g. using the framework of the affine process, see [5]. Then, we only need to substitute $u + i$ for u in the characteristic function of X_t to calculate $CF(t, i + u|X_0, \kappa, \mu, \sigma)$ which is given by

$$CF(t, i + u|X_0, \kappa, \mu, \sigma) = e^{-A(t) - \frac{B(t)}{2} + iu(A(t) + B(t)) + u^2 \frac{B(t)}{2}}, \tag{6}$$

with

$$A(t) = e^{-\kappa t}X_0 + \mu(1 - e^{-\kappa t}), \quad B(t) = -\frac{\sigma^2}{2\kappa}(1 - e^{-2\kappa t}) \tag{7}$$

Finally, the dynamic correlation function $\bar{\rho}_t$ can be computed by

$$\bar{\rho}_t = 1 - \frac{e^{-A(t) - \frac{B(t)}{2}}}{2} \int_{-\infty}^{\infty} \frac{1}{\cosh(\frac{\pi u}{2})} \cdot e^{iu(A(t)+B(t))+u^2 \frac{B(t)}{2}} du, \tag{8}$$

where $A(t)$ and $B(t)$ are defined in (7). In fact, X_0 in $A(t)$ is equal to $\mathrm{artanh}(\bar{\rho}_0)$.

To illustrate the role of each parameter in (8), we plot $\bar{\rho}_t$ for several values of the parameters. First in Fig. 1, we let $\kappa = 2$ and $\sigma = 0.5$ and display $\bar{\rho}_t$ with different values of μ, which is set to be 0.5, 0, and -0.5, respectively. Obviously, μ determines the long term mean of $\bar{\rho}_t$. However, μ is not the exact limiting value. Considering Fig. 1a where the initial value of the correlation function is 0, we see that $\bar{\rho}_t$ is increasing to a value around $\mu = 0.5$ and decreasing to a value around $\mu = -0.5$ as t become larger, when $\mu = 0.5$ and -0.5, respectively. Besides, for $\mu = \bar{\rho}_0 = 0$ we observe that the correlation function $\bar{\rho}_t$ yields always 0 which is the same as constant correlation $\rho = 0$. Now, we set $\bar{\rho}_0 = 0.3$ and keep the value of all other parameters unchanged, then display the curves of $\bar{\rho}_t$ in Fig. 1b.

Next, we fix $\kappa = 2$ and $\mu = 0.5$ and then display $\bar{\rho}_t$ for the varying $\sigma = 0.5$, 1 and 2 in Fig. 2. Obviously, σ shows the magnitude of variation from the transformed mean value of X_t ($\mu = 0.5$). In Fig. 2a we see, the larger the value of σ is, the stronger the deviations of $\bar{\rho}_t$ is from the transformed mean value of X_t. More interesting is that $\bar{\rho}_t$ first decreases until $t \approx 0.25$, then increases and converges to a value, see Fig. 2b where $\bar{\rho}_0 = 0.3$ and $\sigma = 2$.
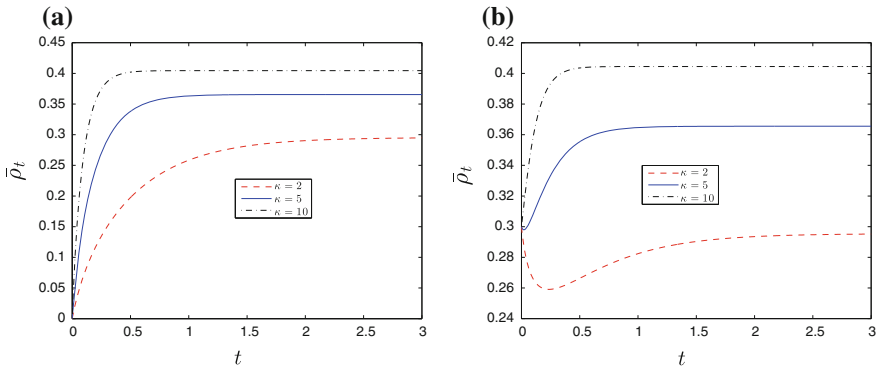
Again, in order to illustrate the role of κ, we set $\mu = 0.5$, $\sigma = 2$ and vary the value of κ, see Fig. 3. From Fig. 3a it is easy to observe that κ represents the speed of $\bar{\rho}_t$ tending to its limit. Especially, as we have seen in Fig. 2b, the curve is more
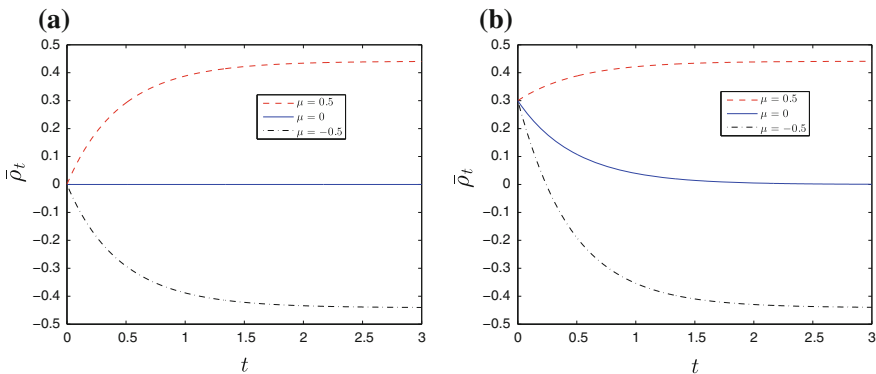
Fig. 1 Dynamic correlation $\bar{\rho}_t$ for varying μ ($\kappa = 2$ and $\sigma = 0.5$). **a** $\bar{\rho}_0 = 0$. **b** $\bar{\rho}_0 = 0.3$
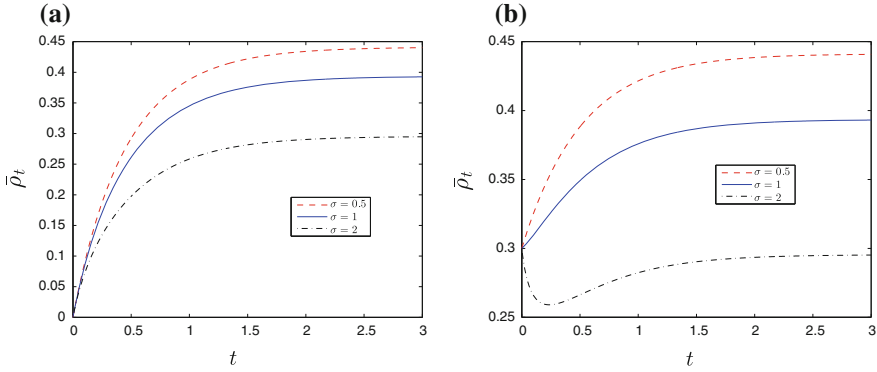
Fig. 2 Dynamic correlation $\bar{\rho}_t$ for varying σ ($\kappa = 2$ and $\mu = 0.5$). **a** $\bar{\rho}_0 = 0$. **b** $\bar{\rho}_0 = 0.3$

Fig. 3 Dynamic correlation $\bar{\rho}_t$ for varying κ ($\mu = 0.5$ and $\sigma = 2$). **a** $\bar{\rho}_0 = 0$. **b** $\bar{\rho}_0 = 0.3$

unstable for $\kappa = 2$ and $\sigma = 2$ in Fig. 3b. However, if σ remains constant while the value of κ is increased, we can see that curves of $\bar{\rho}_t$ become more stable and tend straightly to its limit. If one incorporates the dynamic correlation function (8) to a financial model, the parameter $\bar{\rho}_0$, κ, μ, and σ could be estimated by fitting the model to market data.

3 Dynamically Correlated BMs and Their Construction

We fix a probability space $(\Omega, \mathscr{F}, \mathbb{P})$ and an information filtration $(\mathscr{F}_t)_{t \in \mathbb{R}^+}$, satisfying the usual conditions, see e.g. [11]. At a time $t > 0$, the correlation coefficient of two Brownian motions (BMs) W_t^1 and W_t^2 is defined as

$$\rho_t^{1,2} = \frac{E\left[W_t^1 W_t^2\right]}{t}. \tag{9}$$

If we assume that $\rho_t^{1,2}$ is constant, $\rho_t^{1,2} = \rho^{1,2}$ for all $t > 0$, say W_t^1 and W_t^2 are correlated with the constant $\rho^{1,2}$.

Therefore, we give the definition of dynamically correlated BMs.

Definition 1 Two Brownian motions W_t^1 and W_t^2 are called *dynamically correlated* with correlation function ρ_t, if they satisfy

$$E\left[W_t^1 W_t^2\right] = \int_0^t \rho_s ds, \tag{10}$$

where $\rho_t : [0, t] \to [-1, 1]$. The *average correlation* of W_t^1 and W_t^2, ρ_{Av}, is given by $\rho_{Av} := \frac{1}{t} \int_0^t \rho_s ds$.

We consider first the two-dimensional case and let ρ_t be a correlation function. For two independent BMs W_t^1 and W_t^3 we define

$$W_t^2 = \int_0^t \rho_s dW_s^1 + \int_0^t \sqrt{1 - \rho_s^2}\, dW_s^3, \tag{11}$$

with the symbolic expression

$$dW_t^2 = \rho_t dW_t^1 + \sqrt{1 - \rho_t^2}\, dW_t^3. \tag{12}$$

It can be easily verified that W_t^2 is a BM and correlated with W_t^1 dynamically by ρ_t. Besides, the covariance matrix and the average correlation matrix of $\mathbb{W}_t = (W_t^1, W_t^2)$ can be determined, given by

$$\begin{pmatrix} t & \int_0^t \rho_s ds \\ \int_0^t \rho_s ds & t \end{pmatrix} \quad \text{and} \quad \begin{pmatrix} 1 & \frac{1}{t} \int_0^t \rho_s ds \\ \frac{1}{t} \int_0^t \rho_s ds & 1 \end{pmatrix},$$

respectively.

The construction above could be also generalized to n-dimensions. We denote a standard n-dimensional BM by $\mathbb{Z}_t = (Z_{1,t}, \ldots, Z_{n,t})$ and the matrix of dynamic correlations $\mathscr{R}_t = (\rho_t^{i,j})_{1 < i,j < n}$ which has the Cholesky decomposition for each time t, $\mathscr{R}_t = \mathbb{A}_t \mathbb{A}_t^\top$ with $\mathbb{A}_t = (a_t^{i,j})_{1 < i,j < n}$. We define a new n-dimensional process $\mathbb{W}_t = (W_{1,t}, \ldots, W_{n,t})$ by

$$W_{i,t} = \sum_{j=1}^n a_t^{ij} dZ_{j,t}, \quad i = 1, \ldots, n. \tag{13}$$

We can easily verify that $\mathbb{W}_t$ satisfies the following properties:

- $\mathbb{W}_0 = \mathbf{0}$ and the paths are continuous with probability 1.
- The increments $\mathbb{W}_{t_1} - \mathbb{W}_{t_0}$ and $\mathbb{W}_{t_2} - \mathbb{W}_{t_1}$ are independent for $0 \le t_0 < t_1 < t_2 < t$.
- For $0 \le s < t$, the increment $\mathbb{W}_t - \mathbb{W}_s$ is multivariate normally distributed with mean zero and covariance matrix $\Sigma : \mathbb{W}_t - \mathbb{W}_s \sim N(0, \Sigma)$ with

$$
\Sigma = \begin{pmatrix}
t - s & \int_s^t \rho_u^{1,2} du & \dots & \int_s^t \rho_u^{1,n} du \\
\int_s^t \rho_u^{2,1} du & t - s & \dots & \int_s^t \rho_u^{2,n} du \\
\vdots & \vdots & \ddots & \vdots \\
\int_s^t \rho_u^{n,1} du & \int_s^t \rho_u^{n,2} du & \dots & t - s
\end{pmatrix}.
$$

We call the process $(\mathbb{W}_t)_{t \ge 0}$ *an n-dimensional dynamically correlated Brownian motion,* with the correlation matrix $\mathscr{R}_t$.

4 Dynamic Correlation in the Heston Model

As mentioned before, in many situations the pure Heston model has a limitation on reproducing properly a volatility smile. For this problem, several time-dependent Heston models have been proposed for good fitting to implied volatilities, e.g. [6] and [10]. In this section, we show how to incorporate our time-dependent correlation function into the Heston model.

4.1 Incorporating Dynamic Correlations

Heston's stochastic volatility model is specified as

$$
dS_t = \mu_S S_t dt + \sqrt{v_t}\, S_t\, dW_t^S, \tag{14}
$$
$$
dv_t = \kappa_v(\mu_v - v_t)dt + \sigma_v \sqrt{v_t}\, dW_t^v, \tag{15}
$$

where (14) is the price of the spot asset, (15) is the volatility (variance) and W_t^S and W_t^v are correlated with a constant correlation ρ_{Sv}. To incorporate the time-dependent correlations, we assume that dS_t and dv_t are correlated by a time-dependent correlation function $\bar{\rho}_t$ instead of the constant correlation ρ_{Sv}. The extended Heston model with dynamic correlation $\bar{\rho}$ is specified as

$$
dS_t = \mu_S S_t dt + \sqrt{v_t}\, S_t\, dW_t^1, \tag{16}
$$
$$
dv_t = \kappa_v(\mu_v - v_t)dt + \sigma_v \sqrt{v_t} \left(\bar{\rho}_t\, dW_t^1 + \sqrt{1 - \bar{\rho}_t^2}\, dW_t^2 \right), \tag{17}
$$

where W_t^1 and W_t^2 are independent. Applying Itô's lemma and no-arbitrage arguments yields [9]

$$\frac{1}{2} v S^2 \frac{\partial^2 U}{\partial S^2} + \bar{\rho}_t \sigma_v v S \frac{\partial^2 U}{\partial S \partial v} + \frac{1}{2} \sigma_v^2 v \frac{\partial^2 U}{\partial v^2} + r S \frac{\partial U}{\partial S}$$
$$+ [\kappa_v(\mu_v - v) - \tilde{\lambda}(S, v, \bar{\rho}, t) v] \frac{\partial U}{\partial v} - r U + \frac{\partial U}{\partial t} = 0, \qquad (18)$$

where $\bar{\rho}_t$ is defined in (8) but with the parameter $\bar{\rho}_0$, κ_ρ, μ_ρ, and v_ρ. It is worth mentioning that the market price of volatility risk depends also on the dynamic correlation, which could be written as $\tilde{\lambda}(S, v, \bar{\rho}_t, t)$. This means, the price of correlation risk embedding in the price of volatility risk has been considered.

We consider, e.g. a European call option with strike price K and maturity T in the Heston model

$$C(S, v, t, \bar{\rho}_t) = S P_1 - K P(t, T) P_2, \quad \tau = T - t, \qquad (19)$$

where $P(t, T)$ is the discount factor and both in-the-money probabilities P_1, P_2 must satisfy the PDE (18) as well as their characteristic functions, $f_1(S_t, v_t, \bar{\rho}_t, \phi, t)$ and $f_2(S_t, v_t, \bar{\rho}_t, \phi, t)$

$$f_j(S_t, v_t, \bar{\rho}_t, \phi, t) = E[e^{i\phi \ln S_T} | S_t, v_t, \bar{\rho}_t] = e^{C_j(\tau, \phi) + D_j(\tau, \phi) v + i\phi \ln S_t}, \quad j = 1, 2, \quad (20)$$

where $C_j(0, \phi) = 0$ and $D_j(0, \phi) = 0$. By substituting this functional form (20) into the PDE (18) we can obtain the following ordinary differential equations (ODEs) for the unknown functions C and D:

$$-\frac{1}{2} \phi^2 + \bar{\rho}_t \sigma_v \phi i D_j + \frac{1}{2} \sigma_v^2 D_j^2 + u_j \phi i - b_j D_j + \frac{\partial D_j}{\partial t} = 0, \qquad (21)$$

$$r \phi i + \kappa_v \mu_v D_j + \frac{\partial C_j}{\partial t} = 0, \qquad (22)$$

with the initial conditions $C_j(0, \phi) = D_j(0, \phi) = 0$

$$u_1 = 0.5, \quad u_2 = -0.5, \quad b_1 = \kappa_v + \lambda - \bar{\rho}_t \sigma_v \quad \text{and} \quad b_2 = \kappa_v + \lambda, \qquad (23)$$
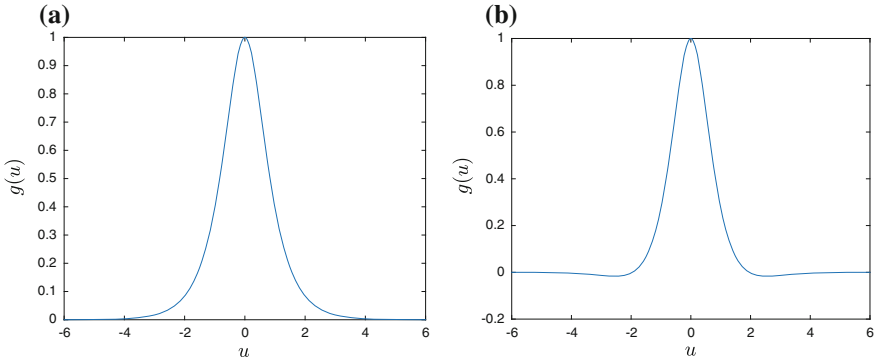
where

$$\bar{\rho}_t = 1 - \frac{e^{-A(t) - \frac{B(t)}{2}}}{2} \int_{-\infty}^{\infty} \underbrace{\frac{1}{\cosh(\frac{\pi u}{2})} \cdot e^{iu(A(t) + B(t)) + u^2 \frac{B(t)}{2}}}_{:= g(u)} \, du, \qquad (24)$$

with $A(t) = e^{-\kappa_\rho t} \text{artanh}(\bar{\rho}_0) + \mu_\rho(1 - e^{-\kappa_\rho t})$, $B(t) = -\frac{\sigma_\rho^2}{2\kappa_\rho}(1 - e^{-2\kappa_\rho t})$.

Obviously, (21) and (22) cannot be solved analytically. Therefore, we need to find an efficient way to compute the option price numerically. We firstly generate the

(a)

(b)

Fig. 4 $g(u)$ under $\rho_0 = 0.3$, $\kappa_\rho = 2$, $\mu_\rho = -0.8$, $\sigma_\rho = 0.1$. **a** $t = 0.1$. **b** $t = 10$

dynamic correlations using (24). We observe that $g(u)$ is a symmetric function about $u = 0$ and vanishes (approaches zero) for a sufficiently large absolute value of u, see Fig. 4. For these two reasons, the numerical integration in (24) is computationally fast. Next we use an explicit Runge–Kutta method, the matlab routine `ode45`, to obtain C and D in (21) and (22) and thus also the characteristic functions (20). Finally, we employ the COS method [8] to obtain the option price $C(S, v, t, \bar{\rho})$ in (19). Thanks to the COS method, although we solved that ODE system numerically, the time for obtaining European option prices is less than 0.1 s so that a calibration can be performed. Obviously, the error consists of the error using `ode45` for (21) and (22) and the error using COS method. The detailed analysis of error using COS method has been provided in [8].

4.2 Calibration of the Heston Model Under Dynamic Correlation

In this section we calibrate the Heston model extended by our time-dependent correlation function to the real market data (Nikk300 index call options on July 16, 2012) and compare these to the pure Heston model [9] and the time-dependent Heston model [10].

We consider a set of N maturities T_i, $i = 1, \ldots, N$ and a set of M strikes K_j, $j = 1, \ldots, M$. Then for each combination of maturity and strike we have a market price $V^M(T_i, K_j) = V_{ij}^M$ and a corresponding model price $V(T_i, K_j; \Theta) = V_{ij}^\Theta$ generated by using (19). We choose the relative mean error sum of squares (RMSE) for the loss function $\frac{1}{M \times N} \sum_{i,j} \frac{(V_{ij}^M - V_{ij}^\Theta)^2}{V_{ij}^M}$, which can be minimized to obtain the parameter estimates

$$\hat{\Theta} = \arg\min \frac{1}{M \times N} \sum_{i,j} \frac{(V_{ij}^M - V_{ij}^\Theta)^2}{V_{ij}^M}. \tag{25}$$

For the optimization we restrict $\bar{\rho}_0$ to the interval $(-1, 1)$ but not the value of μ_ρ. Since it is not the direct limit of the correlation function but the mean reversion of the Ornstein–Uhlenbeck process, thus, it could take any value in $\mathbb{R}$. Our experiments showed, that it is sufficient and appropriate to restrict μ_ρ to the interval $[-4, 4]$.

We state our estimated parameters and the estimation error for the pure Heston model (abbr. PH), the Heston model under our time-dependent correlations (CH), the time-dependent Heston model by Mikhailov and Ngel [10] (MN) in Tables 1, 2 and 3, respectively. We see that the estimation error using the CH model is significantly less than the error using the PH model and almost the same to the error (sum of errors for each maturity) under the MN model. To illustrate more clearly, for each maturity we compare the implied volatilities for all the models to the market volatilities in Fig. 5. We can observe that the implied volatilities for the CH model are much closer to the market volatilities than the implied volatilities for the PH model, especially the CH model has better volatility smile for the short maturity $T = 1/12$. Compared to the MN model, the implied volatilities for our model are almost the same. However, our CH model has an economic interpretation, namely the correlation is nonlinear

Table 1 The estimated parameters for the pure Heston model using call options on the Nikk300 index on July 16, 2012 for the maturities 1/12, 1/4, 1/2, 1

The pure heston model					
$\hat{v}_0$	$\hat{\kappa}_v$	$\hat{\mu}_v$	$\hat{\sigma}_v$	$\hat{\rho}$	Estimation error
0.029	4.746	0.053	1.108	-0.355	1.10×10^{-3}

Table 2 The estimated parameters for the Heston model under time-dependent correlations using call options on the Nikk300 index on July 16, 2012 for the maturities 1/12, 1/4, 1/2, 1
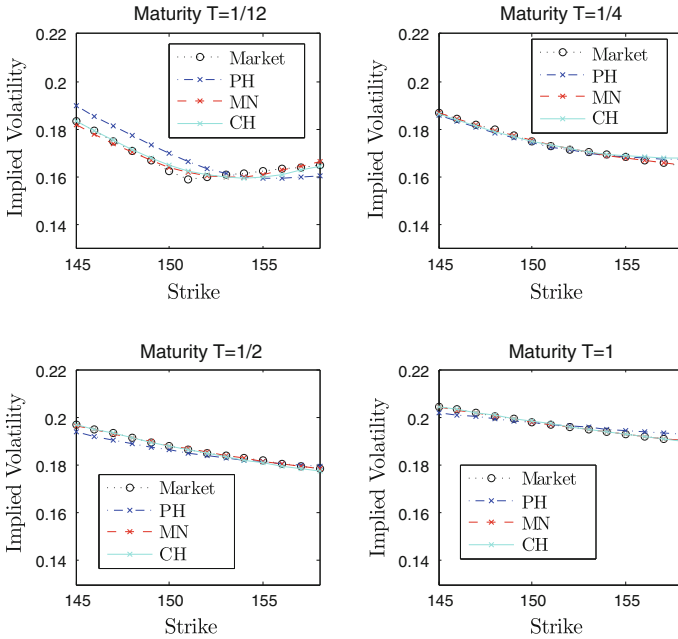
The extended Heston model by using our time-dependent correlation function								
$\hat{v}_0$	$\hat{\kappa}_v$	$\hat{\mu}_v$	$\hat{\sigma}_v$	$\hat{\bar{\rho}}_0$	$\hat{\kappa}_\rho$	$\hat{\mu}_\rho$	$\hat{\sigma}_\rho$	Estimation error
0.027	5.542	0.055	1.224	-0.165	5.333	-0.752	0.434	2.38×10^{-4}

Table 3 The estimated parameters for the time-dependent Heston model by Mikhailov and Ngel using call options on the Nikk300 index on July 16, 2012

The time-dependent Heston model by Mikhailov and Ngel						
Maturity	$\hat{v}_0$	$\hat{\kappa}_v$	$\hat{\mu}_v$	$\hat{\sigma}_v$	$\hat{\rho}$	Estimation error
1/12	0.025	2.749	0.095	1.172	-0.201	1.78×10^{-4}
1/4	0.012	2.936	0.076	0.524	-0.411	2.45×10^{-5}
1/2	0.011	2.890	0.058	0.592	-0.430	1.14×10^{-5}
1	0.001	2.911	0.051	0.558	-0.389	4.28×10^{-6}

Fig. 5 The comparison of implied volatilities for all the models to the market volatilities of the call options on the Nikk300 index on July 16, 2012, where the spot price is 150.9

and time-dependent as market requires. We conclude that the Heston model extended by incorporating our time-dependent correlations can provide better volatility smiles compared to the pure Heston model. The time-dependent correlation function can be easily and directly introduced into the financial models.

5 Conclusion

In this work, we first investigated the dynamically (time-dependent) correlated Brownian motions and their construction. Furthermore, we proposed a new dynamic correlation function which can be easily incorporated into another financial model. The aim of using our dynamic correlation function is to reasonably choose additional parameters to increase the fitting quality on the one-hand side, but also add an economically meaningful perspective.

As an application, we incorporated our time-dependent correlation function into the Heston model. An experiment on estimation of the models using real market data has been provided. The numerical calibration results show that the Heston model extended by using our time-dependent correlation function provides better volatility

smiles compared to the pure Heston model. Besides, this time-dependent correlation function could be easily and directly imposed to the financial models and thus it is preferred to use instead of a constant correlation.

References

1. Brigo, D., Capponi, A.: Bilateral counterparty risk with application to CDSs. Risk Mag. **23**(3), 85–90 (2010)
2. Brigo, D., Chourdakis, K.: Counterparty risk for credit default swaps: impact of spread volatility and default correlation. Int. J. Theoret. Appl. Financ. **12**, 1007–1026 (2009)
3. Campbell, J., Lo, A., MacKinlay, A.: The Econometrics of Financial Markets. Princeton University Press, Princeton (1997)
4. Chen, H., Joslin, S.: Generalized transform analysis of affine processes and applications in finance. Rev. Fin. Stud. **25**(7), 2225–2256 (2012)
5. Duffie, D., Filipović, D., Schachermayer, W.: Affine processes and applications in finance. Ann. Appl. Probab. **13**(3), 984–1053 (2003)
6. Elices, A.: Affine concatenation. Wilmott J. **1**(3), 155–162 (2009)
7. Escobar, M., Götz, B., Neykova, D., Zagst, R.: Stochastic correlation and volatility mean-reversion - empirical motivation and derivatives pricing via perturbation theory. Appl. Math. Fin. **21**(6), 555–594 (2014)
8. Fang, F., Oosterlee, C.W.: A novel pricing method for European options based on Fourier-cosine series expansions. SIAM J. Sci. Comput. **31**, 826–848 (2008)
9. Heston, S.L.: A closed-form solution for options with stochastic volatility with applications to bond and currency options. Rev. Fin. Stud. **6**(2), 327–343 (1993)
10. Mikhailov, S., Nögel, U.: Heston's stochastic volatility model: implementation, calibration and some extensions. Wilmott Mag. 74–79 (2003)
11. Øksendal, B.: Stochastic Differential Equations. Springer, Berlin (2002)
12. Teng, L., Ehrhardt, M., Günther, M.: Bilateral counterparty risk valuation of CDS contracts with simultaneous defaults. Int. J. Theoret. Appl. Financ. **16**(7), 1350040 (2013)

13. Teng, L., van Emmerich, C., Ehrhardt, M., Günther, M.: A versatile approach for stochastic correlation using hyperbolic functions. Int. J. Comput. Math. **93**(3), 524–539 (2016)
14. Uhlenbeck, G.E., Ornstein, L.S.: On the theory of Brownian motion. Phys. Rev. **36**, 823–841 (1930)